Talanta 154 (2016) 455–460

Contents lists available at ScienceDirect

Talanta

journal homepage: www.elsevier.com/locate/talanta

Proximity hybridization-regulated chemiluminescence resonance energy transfer for homogeneous immunoassay

Mengmeng Liu, Jie Wu*, Kaili Yang, Chen Zong, Jianping Lei, Huangxian Ju

State Key Laboratory of Analytical Chemistry for Life Science, School of Chemistry and Chemical Engineering, Nanjing University, Nanjing 210093, China

ARTICLE INFO

Article history:
Received 19 October 2015
Received in revised form
26 January 2016
Accepted 28 January 2016
Available online 29 January 2016

Keywords:
Immunoassay
Proximity hybridization
Chemiluminescence resonance energy transfer
Graphene oxide
CEA

ABSTRACT

Chemiluminescence resonance energy transfer (CRET) and the proximity ligation assay have been widely used in design of sensors for the bioanalysis. Here, a wash-free and homogeneous strategy was proposed to detect carcino-embryonic antigen (CEA) based on proximity hybridization-regulated CRET. The Cy5 demonstrated strong chemiluminescence (CL) via the oxidation of TCPO in the presence of H_2O_2 and energy transfer between excited TCPO and Cy5. Graphene oxide (GO) as an excellent quencher was used to produce the "Signal off" mode that little CL emission was observed through CRET between GO and the Cy5-labelled DNA3. Once CEA was introduced, the target-induced proximity hybridization occurred to form a proximate complex, which inhibited the CRET by preventing GO from absorbing Cy5-labelled DNA3. Furthermore, taking advantage of nicking endonuclease Nt.BbvCI for in situ recycling, the signal could be further amplified for highly sensitive CL detection. Our results showed that this strategy enabled a specific response to CEA with a detection range of 5 orders of magnitude, along with a detection limit of 3.2 pg mL^{-1}. Apart from its easy operation, high sensitivity and acceptable accuracy, the proposed method needed only 0.3 μL of sample, indicating its great opportunity for commercial application.

1. Introduction

The immunoassay is a key technology for clinical diagnostics and environmental testing due to the good specificity [1,2]. Generally, immunoassay methods, including chemiluminescence immunoassays (CLIA) [3,4], enzyme-linked immunosorbent assays (ELISA) [5] and fluoroimmunoassays [6] have been widely used. Combining the specificity of immunoassay and the sensitivity of CL, CLIA possesses have been well established for the quantitation of low concentration analytes in complex samples with the advantages of high sensitivity, high selectivity, low cost and pollution-free [7,8]. For example, our group previously developed a chemiluminescence imaging immunoassay method which could simultaneously and selectively detect 4 tumor markers with the detection limits down to fg mL^{-1} level by using gold nanoparticle-based multienzymatic amplification tags [9]. Traditionally, the analyte molecules in heterogeneous assay formats are accumulated on solid substrates, such as magnetic microparticles and disposable glass chips [10,11], which is time-consuming with washing and separation steps. Thus, no-wash and one-step homogeneous CLIAs are urgently needed for fast and high-throughput detection.

Similar to fluorescence resonance energy transfer (FRET), chemiluminescence resonance energy transfer (CRET) involves non-radiative energy transfer from a chemiluminescent donor to a suitable acceptor molecule [12]. Meanwhile, unlike the FRET, CRET occurs by the oxidation of a luminescent substrate, and then the excited substrate directly transfers the energy to the acceptor without an external excitation source, which avoids photobleaching and autofluorescence [13]. Various nanomaterias have been utilized as the energy acceptor, involving carbon nanoparticles [14–17], quantum dots (QDs) [18,19] and metallic nanomaterials [20–22]. As a single-atom-thick and two-dimensional carbon material, grapheme oxide (GO) has attracted an increasing interest owning to its remarkable characteristics [23]. Moreover, GO could serve as a good energy acceptor due to its excellent quenching efficiency with the long-range nanoscale energy transfer property [24,25]. To the best of our knowledge, there is still no report focusing on the proximity hybridization-regulated GO based CRET for homogeneous detection of protein.

The PLA, which relies on simultaneous recognition of a target molecule by a pair of affinity probes, is a newly developed homogenous DNA-assisted immunoassay [26,27]. Significantly, the bound probes can be functionalized to convert the target event to amplifiable tag sequences for subsequent real-time PCR quantification or localized rolling-circle amplification, which ensures PLA to be one of the most universal and sensitive protein assays [28,29]. In our previous work, several affinity ligand-based

* Corresponding author. Tel./fax: +86 25 83593593.
E-mail address: wujie@nju.edu.cn (J. Wu).

http://dx.doi.org/10.1016/j.talanta.2016.01.060
0039-9140/

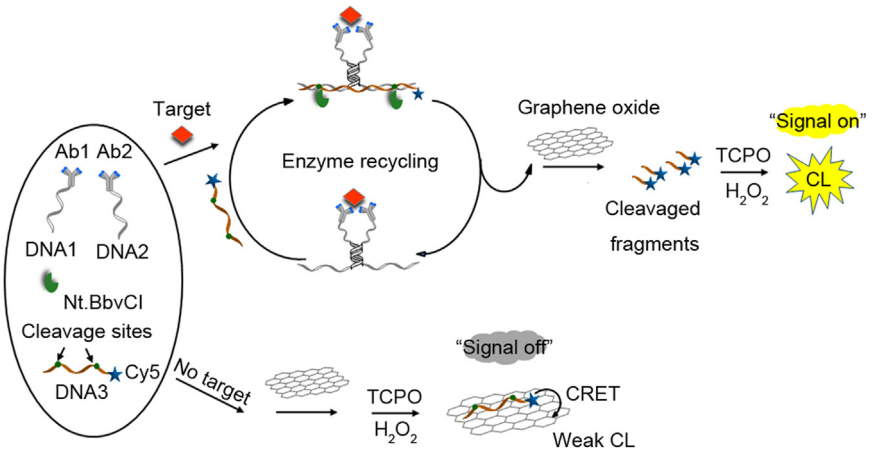

Fig. 1. Schematic illustration of proximity hybridization-regulated CRET for homogeneous detection of CEA.

proximity assay methods have been designed via target-induced DNA assembly and enzymatic amplification cycle for one-step and ultrasensitive detection of protein [30,31]. Yet, these strategies require the DNA to be multi-modified, leading to high-cost as well as complex operation, which makes their application in point-of-care testing remain challenging.

Here, taking advantages of proximity hybridization to regulate the efficiency of CRET, we developed a wash-free and homogeneous immunoassay for CEA detection for the first time (Fig. 1). Firstly, the CL of Cy5 was generated via the oxidation of TCPO in the presence of H_2O_2 and energy transfer between excited TCPO and Cy5. When GO was introduced into this system, the CL of Cy5 attached at the end of single-stranded DNA3 was quenched via CRET. With the adding of target CEA and the antibody-DNA complexes, the target-induced proximity hybridization occurred to form a proximate complex, which inhibited the CRET through desorbing DNA3 from GO. More importantly, a signal amplification strategy was realized by using nicking endonuclease Nt.BbvCI for in situ recycling of the proximity complex. At optimal conditions, this strategy showed a specific response to CEA with a detection range of 5 orders of magnitude, along with a detection limit at pg mL^{-1} level. Our method was successfully applied for determination of CEA levels in serum from cancer patients, and the results were in good agreement with commercial assays.

2. Experimental section

2.1. Materials and reagents

The oligonucleotides were synthesized and HPLC-purified by Sangon Biological Engineering Technology & Co. Ltd. (Shanghai, China). The oligonucleotide sequences were shown in Table S1. CEA, anti-CEA antibody (anti-CEA, mouse monoclonal antibodies, clone nos. Z-2011 and Z-2012) and α-fetoprotein (AFP) were purchased from Keybiotech Co. Ltd. (Beijing, China). Sulfosuccinimidyl-4-(N-maleimidomethyl) cyclohexane-1-car-boxylate (SMCC) was supplied by HeownsBiochem LLC (China), and dithiothreitol (DTT) was from Sangon Biotechnology Co. Ltd. (Shanghai, China). Nt.BbvCI as well as 10 × NEB 2.1 buffer (pH 7.9 at 25 °C) was obtained from New England BioLabs Inc. (USA). Bis(2,4,6-trichlorophenyl) oxalate (TCPO) was purchased from Tokyo Chemical Industry Co. Ltd. (Japan). GO was obtained from XFNano Materials Tech Co. Ltd. (Nanjing, China). All other reagents were of analytical grade and used without further purification. Ultrapure water obtained from a Millipore water purification system (≥ 18 MΩ, Milli-Q, Millipore) was used in all experiments. TE buffer (10 mM, containing 1 mM EDTA and 0.3 M NaCl, pH 7.9) was used as the stock solution for oligonucleotides. PBS1 (55 mM, containing 150 mM NaCl and 20 mM EDTA, pH 7.2) and PBS2 (55 mM, containing 150 mM NaCl and 5 mM EDTA, pH 7.2) were used to prepare DNA-labeled antibodies. NEB buffer 2.1 (1 ×) was used for the homogeneous CL detection of CEA. The clinical serum samples were from Jiangsu Cancer Hospital and stored at −20 °C before use.

2.2. Apparatus

An IFFM-E luminescent analyzer (Remax, Xian, China) was used to collect the CL signal. A F97XP fluorospectophotometer (Lengguang Tech., China) was used to record the FL signal. The gel electrophoresis was performed on the DYCP-31BN electrophoresis analyzer (Liuyi Instrument Company, China) and imaged on a BioradChemDoc XRS (Bio-Rad, USA). The ultraviolet-visible (UV–vis) absorption spectra were recorded with a Nanodrop-2000C UV–vis spectrophotometer (Nanodrop, USA).

2.3. Preparation of DNA-labeled antibody

The DNA-labelled antibody was prepared according to the previous work [32]. 2 mg mL^{-1} Anti-CEA was first reacted with a 20-fold molar excess of SMCC in PBS1 for 2 h at room temperature. At the same time, 12 μL of 100 μM thiolated oligonucleotide (DNA1 or DNA2) was reduced with 16 μL of 100 mM DTT in PBS1 at 37 °C for 1 h. Both products were purified by ultrafiltration (100 KD Millipore for anti-CEA-SMCC and 10 KD Millipore for the reduced oligonucleotide, 10000 rmp, 10 min). After mixing the two reaction products in PBS2 to incubate overnight at 4 °C, the unreacted anti-CEA and DNA were removed by ultra-filtration using a 100 KD millipore (10000 rmp, 10 min) for 3 times, and the obtained Ab-DNA was collected in PBS2.

2.4. Homogeneous CL detection of CEA

The detection was performed by mixing 0.3 μL of 10 μM DNA3 with 1.2 μL of 250 nM Ab1-DNA1 and Ab2-DNA2, 0.25 μL 10000 U mL^{-1} Nt.BbvCI, 0.3 μL of various concentrations of CEA or serum samples and 1 × NEB buffer 2.1 to a total volume of 29.3 μL, followed by a 30 min incubation at 37 °C. Then, 0.7 μL 1 mg mL^{-1} GO solution was added. After 3 min, 20 μL of CL substrate containing 8.5 mM TCPO and 25 mM H_2O_2 was added to record the CL intensity at gain 2 and 950 V.

2.5. Polyacrylamide gel electrophoresis

A 5% native polyacrylamide gel (PAGE) was prepared using 1 × Tris-Borate-EDTA (TBE) buffer. The loading sample was the mixture of 7 μL of DNA or DNA and Nt.BbvCI sample, 1.5 μL of 6 × loading buffer, and 1.5 μL of UltraPowerTM dye and kept for 3 min so that the dye was allowed to integrate with DNA completely. Then the loading sample was injected into polyacrylamide hydrogel. The gel electrophoresis was run at 90 V for 30 min. The resulting board was illuminated with UV light and scanned with a Molecular Imager Gel Doc XR.

3. Results and discussion

3.1. Principle of proximity hybridization-regulated CRET for detection of CEA

A Cy5-labelled DNA3, two antibody-DNA complexes (Ab1-DNA1 and Ab2-DNA2), a nicking enzyme Nt. BbvCI and GO were integrated to perform the strategy as shown in Fig. 1. The DNA3 was designed to contain 2 nicking endonuclease sites and 9 bases that were complementary to DNA1 and DNA2, respectively. In the absence of CEA, DNA 3 was absorbed on GO surface by π-π stacking, and its CL was quenched though CRET [33], denoting as "Signal off". Upon introduction of CEA, the simultaneous recognition of antibody (Ab) in two Ab-DNA complexes to target brought DNA1 and DNA2 in sufficient proximity to form a proximate complex that could hybridize with DNA3. Once duplexes were formed, Nt. BbvCI was employed to cleave on the sites to release the proximity complex which could hybridize with another DNA3 and trigger the second cycle of cleavage. Thus, each proximity complex could produce plentiful Cy5-labelled short DNAs that could hardly be absorbed onto GO to amplify the CL signal [34]. Therefore, based on the proximity hybridization-regulated CRET, a "Signal on" strategy was achieved for a sensitive detection of CEA with high specificity.

3.2. Feasibility of the strategy

The kinetic behavior of the CL signal of the strategy was studied in a static format as shown in Fig. 2A. The CL intensity corresponding to the reaction increased quickly and reached a peak at about 6 s, which ensured the CL intensity to be read out easily. Upon addition of GO into the solution of Cy5 labeled ssDNA (DNA3), the CL intensity greatly decreased (Fig. 2B). The quenching efficiency (QE) of GO on the CL of Cy5 was calculated to be 92.1 ± 0.5%, indicating that strong interaction occurred between GO and DNA3. In the absence of CEA, DNA1 and DNA2 were not close enough to hybridize with each other, leading to the low CL intensity denoted as background (Column 1). On the contrary, the presence of CEA led to the formation of proximate complex, which could not be attached on the surface of GO, and thus produced a signal increase (Column 2). Then, the CL intensity was greatly strengthened with the introduction of the Nt.BbvCI-assisted enzymatic recycling amplification (Fig. 2C). Moreover, the same conclusion has been obtained through measuring fluorescence intensity of the system under different conditions (Fig. 2D).

3.3. Characterization and Optimization of ab-DNA

The signal-to-noise ratio depended largely on the number of complementary bases between DNA1 and DNA2. To simplify the optimization of complementary base number, an 80 nucleotide DNA loop (DNA4) was used to mimic the formation of the proximate complex [35]. As shown in Fig. 3A, 10 and 8 complementary bases (10 bp and 8 bp) caused large noises due to the self-hybridization of DNA1 and DNA2′, which produced a fake proximate effect. Whereas, DNA2′ with 4 bases complementary to DNA1 brought about a rather low signal, suggesting that the proximate complex could not be formed. The noise rather than signal decreased sharply with the decreasing number of complementary bases to 6 bp. According to the maximum signal-to-noise ratio, DNA2′ with 6 bases complementary to DNA1 was chosen for the assay. In order to further testify the proximity hybridization of the optimized strands, PAGE analysis was employed (Fig. S1). The mixture of DNA1, DNA2′, and DNA3 (lane 4) showed a band at the

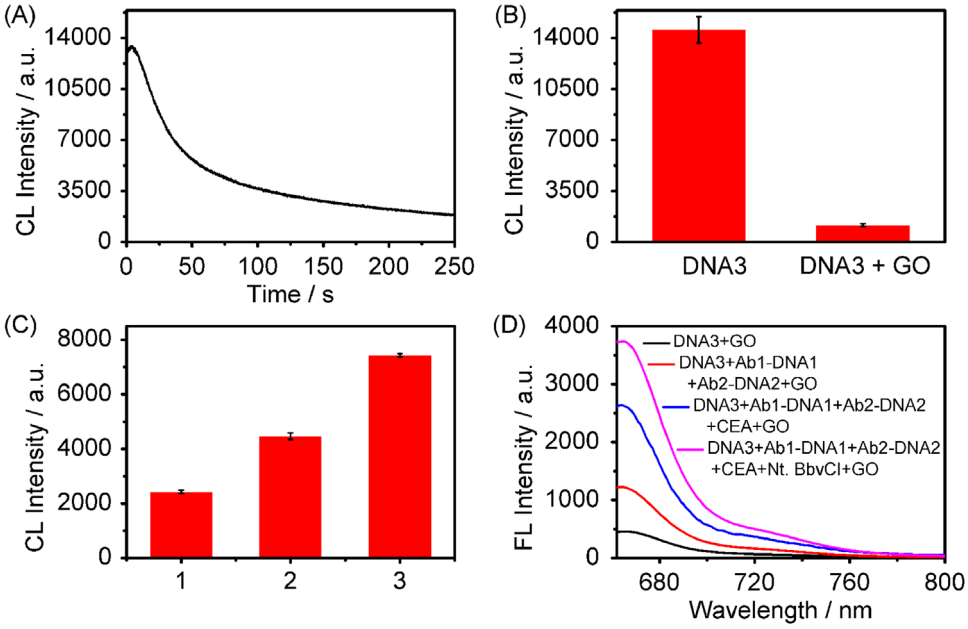

Fig. 2. (A) Kinetic curve of the CL reaction at 100 nM DNA3. (B) CL Intensity of 100 nM DNA3 with and without GO. (C) CL intensity for the mixture of (1) DNA3 + Ab1-DNA1 + Ab2-DNA2 + GO, (2) (1) + 100 ng mL^{-1} CEA, (3) (2) + 2.5 U of Nt. BbvCI. (D) Fluorescent spectra of different solutions containing the marked components.

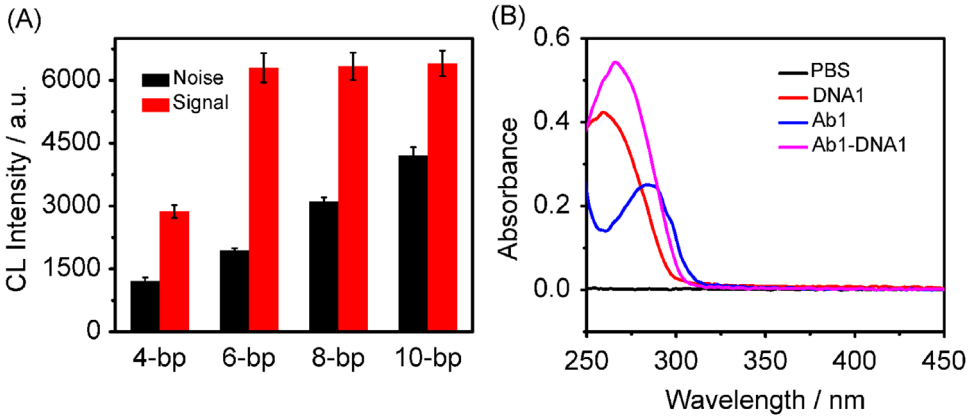

Fig. 3. (A) Optimization of complementary base number between DNA1 and DNA2. (B) Absorption spectra of PBS, anti-CEA, DNA1 and the conjugation products.

same position as DNA1 (lane 3), suggesting that no hybridization among DNA1, DNA2′, and DNA3 occurred. Once DNA4 was added, there showed a new band at ~180 bp (lane 5), which indicated that DNA1, DNA2′, DNA3, and DNA4 hybridized to form the proximate complex of DNA1/DNA4/DNA2′/DNA3 (lane 6). After introducing Nt.BbvCI to this mixture, the bands occurred at the same position with proximate complex in lane 5 (lane 7), which could be attributed to the cleavage of DNA3 from DNA1/DNA4/DNA2′/DNA3.

Through measuring the UV–vis absorbance of Ab-DNA at 260 and 280 nm (Fig. 3B) of DNA [36], the molecular ratio of DNA versus antibody was calculated to be about 5 on the basis of the absorbance ratio (260 vs 280 nm). In addition, by comparing the UV–vis absorbance of DNA before and after reaction to form Ab-DNA (Fig. S2), it could be figured out around 5 DNA strands on each Ab, which was consistent with the above method.

3.4. Optimization of detection conditions

In order to achieve the optimal detection performance, the concentration of GO as a critical factor for detection efficiency was firstly optimized. As shown in Fig. 4A, the CL intensity decreased by 90% as the concentration of GO increased to 23.3 μg mL^{-1}, which was chosen for CEA detection. Since the proposed assay employed an in situ enzymatic recycling amplification, the concentration of Nt.BbvCI was also optimized. The noise was slightly changed with the increase of the concentration of Nt.BbvCI, which led to a high efficiency of signal amplification. On the other hand, the CL intensity at 2.5 U of Nt.BbvCI concentration was 2.9 times of that in the absence of Nt.BbvCI (Fig. 4B). What's more, the reaction time was another important factor affecting the assay performance. It was obvious that with reaction time rising, the CL intensity increased and reached a plateau at 30 min, which led to an optimal incubation time of 30 min for obtaining the highest ratio of signal-to-noise (Fig. 4C). Since the H_2O_2 concentration would strongly affect the CL intensity, it was investigated and an optimal concentration of 25 mM was chosen to obtain the highest ratio of signal-to-noise (Fig. 4D).

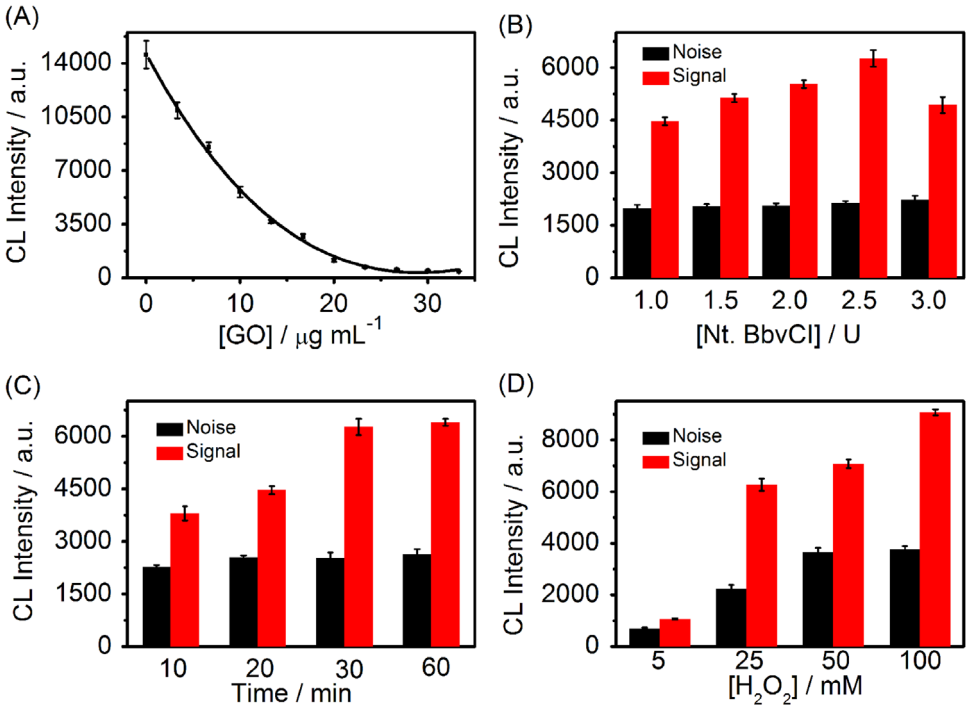

Fig. 4. (A) Effects of GO concentration on CL intensity for 100 mM DNA3. Optimization of (B) concentration of Nt. BbvCI, (C) incubation time and (D) H_2O_2 concentration for the strategy at 10 ng mL^{-1} CEA.

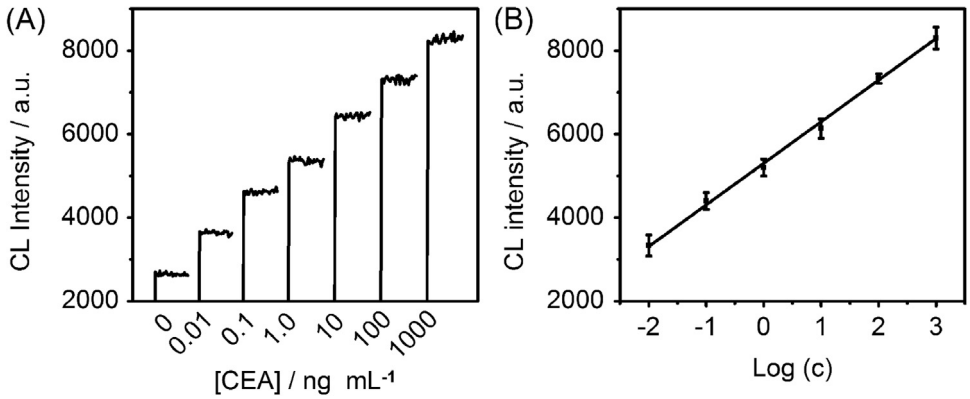

Fig. 5. (A) CL response to CEA at 0, 0.01, 0.1, 1.0, 10, 100 and 1000 ng mL^{-1}. (B) Calibration curve for CEA detection.

3.5. Analytical performance

Under the optimal conditions, the CL intensity increased with the increasing CEA concentration (Fig. 5A), linearly depending on the logarithm of CEA concentration in the range of 1.0×10^{-2} to 1.0×10^{3} ng mL^{-1} with a correlation coefficient of 0.9965 (Fig. 5B). Corresponding to the signal of 3 times the standard deviation, the limit of detection for CEA was 3.2 pg mL^{-1} (~ 10 fM), which was lower than those of conventional immunoassays [37,38] and was comparable to other CRET [16,39] or proximity dependent methods [40]. Owning to simultaneous recognition of target protein by a pair of PLA probes and the strong CL quenching effect of GO, the proposed method possessed high sensitivity and a wide detection range.

AFP and CEA are most common tumor markers and usually coexist in real biological samples. The selectivity of the proposed method was evaluated by comparing CL intensity of the solutions containing either CEA or AFP, and the mixture of CEA and AFP. As shown in Fig. 6, only CEA or the mixture of CEA and AFP caused obvious CL increase, while the influence of AFP was negligible. Such results indicated that the proposed method demonstrated a high specificity for CEA, which was attributed to the specific recognition of a pair of PLA probes to CEA.

3.6. Real sample analysis

To assess the application of the proposed method in complex biological systems, the analysis of CEA in clinical serum samples was carried out. The assay results in five clinical serum samples

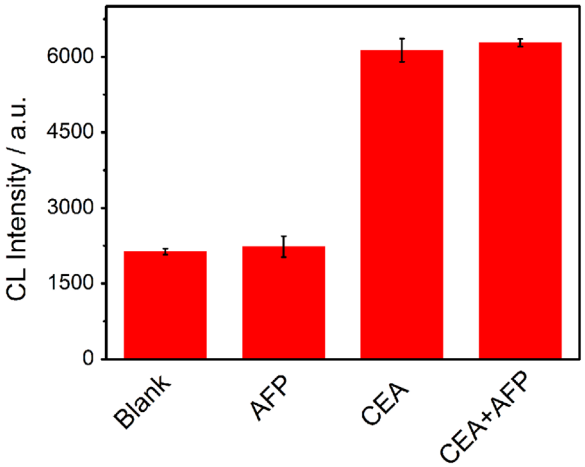

Fig. 6. Specificity of the proposed method using 10 ng mL^{-1} AFP, 10 ng mL^{-1} CEA and 10 ng mL^{-1} CEA + 10 ng mL^{-1} AFP.

Table 1
Assay results of CEA in clinical serum samples using the proposed and reference methods.

Sample no	Proposed method (ng mL^{-1})	Reference method (ng mL^{-1})	Relative error (%)
1	1.38	1.48	−6.67
2	9.47	9.19	3.05
3	45.95	43.10	6.61
4	140.5	148.9	−5.64
5	453.2	479.8	−5.54

were in good agreement with the reference values from the commercial electrochemiluminescent testing as shown in Table 1. In general, relative errors less than 6.67% indicated the method possessed excellent reliability. Additional, the presented method could be a powerful protocol for point-of-care analysis by coupling with the flow-injection system for automatic sampling and the photomultiplier for sensitive signal record.

4. Conclusions

In summary, this work developed a proximity hybridization-regulated CRET strategy for homogeneous protein detection. The CL of Cy5 was demonstrated via the green reaction using TCPO and H_2O_2 as substrate. Instead of simultaneous modification of both luminophore and quencher, GO was introduced to perform as the energy acceptor, making this strategy more universal. Besides, owning to the requirement of two simultaneous binding events for a single target molecule as well as endonuclease recycling amplification, the proposed method possessed high sensitivity and selectivity. Taking CEA as a model target, the assay showed a wide detection range, low limit of detection, and acceptable accuracy. By simple incorporation of the corresponding binding molecules, the proximity hybridization-regulated CRET assay could be easily extended to other biological molecules as a universal method.

Acknowledgements

This work was supported by National Natural Science Foundation of China (21105046), PhD Fund for Young Teachers (20110091120012), and Natural Science Foundation of Jiangsu (BK2011552).

Appendix A. Supplementary material

Supplementary data associated with this article can be found in the online version at http://dx.doi.org/10.1016/j.talanta.2016.01.060.

References

[1] X. Liu, Q. Dai, L. Austin, J. Coutts, G. Knowles, J.H. Zou, H. Chen, Q. Huo, J. Am. Chem. Soc. 130 (2008) 2780–2782.
[2] Y. Date, A. Aota, K. Sasaki, Y. Namiki, N. Matsumoto, Y. Watanabe, N. Ohmura, T. Matsue, Anal. Chem. 86 (2014) 2989–2996.
[3] H. Akhavan-Tafti, D.G. Binger, J.J. Blackwood, Y. Chen, R.S. Creager, R. de Silva, R.A. Eickholt, J.E. Gaibor, R.S. Handley, K.P. Kapsner, S.K. Lopac, M.E. Mazelis, T. L. McLernon, J.D. Mendoza, B.H. Odegaard, S.G. Reddy, M. Salvati, B. A. Schoenfelner, N. Shapir, K.R. Shelly, J.C. Todtleben, G.P. Wang, W.H. Xie, J. Am. Chem. Soc. 135 (2013) 4191–4194.
[4] I. Al-Ogaidi, H.L. Gou, Z.P. Aguilar, S.W. Guo, A.K. Melconian, A.K.A. Al-kazaz, F. K. Meng, N.Q. Wu, Chem. Commun. 50 (2014) 1344–1346.
[5] B.Y. Cao, G.Z. He, H. Yang, H.F. Chang, S.Q. Li, A.P. Deng, Talanta 115 (2013) 624–630.
[6] R. Charlermroj, O. Himananto, C. Seepiban, M. Kumpoosiri, N. Warin, O. Gajanandana, C.T. Elliott, N. Karoonuthaisiri, Anal. Chem. 86 (2014) 7049–7056.
[7] T.B. Xin, H. Chen, Z. Lin, S.X. Liang, J.M. Lin, Talanta 82 (2010) 1472–1477.
[8] Y.M. Liu, L. Mei, L.J. Liu, L.F. Peng, Y.H. Chen, S.W. Ren, Anal. Chem. 83 (2011) 1137–1143.
[9] C. Zong, J. Wu, C. Wang, H.X. Ju, F. Yan, Anal. Chem. 84 (2012) 2410–2415.
[10] B. Sai, Zh.P. Zhang, Y. Dong, Z.H. Wang, Biosens. Bioelectron 65 (2015) 139–144.
[11] C. Zong, J. Wu, J. Xu, H.X. Ju, F. Yan, Biosens. Bioelectron 43 (2013) 372–378.
[12] X.Y. Huang, L. Li, H.F. Qian, C.Q. Dong, J.C. Ren, Angew. Chem. Int. Ed. 45 (2006) 5140–5143.
[13] S.L. Zhao, Y. Huang, R.J. Liu, M. Shi, Y.M. Liu, Chem. Eur. J 16 (2010) 6142–6145.
[14] Z.X. Wang, H.F. Gao, Z.F. Fu, Analyst 138 (2013) 6753–6758.
[15] Z. Lin, X.N. Dou, H.F. Li, Y. Ma, J.M. Lin, Talanta 132 (2015) 457–462.
[16] Z.M. Zhou, Z. Feng, J. Zhou, B.Y. Fang, X.X. Qi, Z.Y. Ma, B. Liu, Y.D. Zhao, X.B. Hu, Biosens. Bioelectron 64 (2015) 493–498.
[17] H.F. Gao, W.W. Wang, Z.X. Wang, J. Han, Z.F. Fu, Anal. Chim. Acta 819 (2014) 102–107.
[18] R. Freeman, X.Q. Liu, I. Willner, J. Am. Chem. Soc. 133 (2011) 11597–11604.
[19] X.Q. Liu, R. Freeman, E. Golub, I. Willner, ACS Nano 5 (2011) 7648–7655.
[20] D.G. He, X.X. He, K.M. Wang, X. Yang, X.X. Yang, X.C. Li, Z. Zou, Chem. Commun 50 (2014) 11049–11052.
[21] X.Y. Huang, J.C. Ren, Anal. Chim. Acta 686 (2011) 115–120.
[22] J.X. Du, Y.D. Wang, W.M. Zhang, Chem. Eur. J 18 (2012) 8540–8546.
[23] K.P. Loh, Q.L. Bao, G. Eda, M. Chhowalla, Nat. Chem. 2 (2010) 1015–1024.
[24] R.S. Swathi, K.L. Sebastian, J. Chem. Phys. 130 (2009) 086101.
[25] S. Bi, T.T. Zhao, B.Y. Luo, Chem. Commun 48 (2012) 106–108.
[26] J. Kim, J.M. Hu, R.S. Sollie, C.J. Easley, Anal. Chem. 82 (2010) 6976–6982.
[27] X.X. Gao, R.N. Hannoush, J. Am. Chem. Soc. 136 (2014) 4544–4550.
[28] S. Fredriksson, W. Dixon, H. Ji, A.C. Koong, M. Mindrinos, R.W. Davis, Nat. Methods 4 (2007) 327–329.
[29] Y.L. Wei, W.J. Zhou, J. Liu., Y.Q. Chai, Y. Xiang, R. Yuan, Talanta 141 (2015) 230–234.
[30] C. Zong, J. Wu, M.M. Liu, L.L. Yang, L. Liu, F. Yan, H.X. Ju, Anal. Chem. 86 (2014) 5573–5578.
[31] K.W. Ren, J. Wu, F. Yan, H.X. Ju, Sci. Rep. 4 (2014) 4360.
[32] O. Söderberg, M. Gullberg, M. Jarvius, K. Ridderstråle, K.J. Leuchowius, J. Jarvius, K. Wester, P. Hydbring, F. Bahram, L.G. Larsson, U. Landegren, Nat. Methods, 12, (2006) 995–1000.
[33] N. Varghese, U. Mogera, A. Govindaraj, A. Das, P.K. Maiti, A.K. Sood, C.N.R. Rao, ChemPhysChem 10 (2009) 206–210.
[34] P.J.J. Huang, J.W. Liu, Small 8 (2012) 977–983.
[35] J.M. Hu, T.Y. Wang, J. Kim, C. Shannon, C.J. Easley, J. Am. Chem. Soc. 134 (2012) 7066–7072.
[36] Z.J. Zhou, Y. Xiang, A.J. Tong, Y. Lu, Anal. Chem. 86 (2014) 3869–3875.
[37] Q.L. Yu, X.F. Zhan, K.P. Liu, H. Lv, Y.X. Duan, Anal. Chem. 85 (2013) 4578–4585.
[38] C.H. Zhou, J.Y. Zhao, D.W. Pang, Z.L. Zhang, Anal. Chem. 86 (2014) 2752–2759.
[39] Z.M. Zhou, J. Zhou, J. Chen, R.N. Yu, M.Z. Zhang, J.T. Song, Y.D. Zhao, Biosens. Bioelectron. 59 (2014) 397–403.
[40] B. Deng, J.B. Chen, H.Q. Zhang, Anal. Chem. 86 (2014) 7009–7016.